

Impaired neurodevelopment by the low complexity domain of CPEB4 reveals a convergent pathway with neurodegeneration

Jihae Shin¹, Johnny S. Salameh², and Joel D. Richter^{1*}

¹Program in Molecular Medicine

²Department of Neurology

University of Massachusetts Medical School

Figure S1, related to Figure 2

A

1	MGDYGFGVLVQSNTGNKSAFPVRFPHLQPPHHHQNATPSAAFINNNTAANGSSAGSAW
61	LFPAPATHNIQDEILGSEKAKSQQQEQQDPLEKQQLSPSPGQEAGILPETEKAKSEENQG
121	DNSSENGNGKEKIRIESPVLTGF DYQEATGLGTSTQPLTSSASSLTGFSNWSAAIAPSSS
181	TIINEDASFFHQGGVPAASANNGALLFQNFPHHVSPGFGGSFSPQIGPLSQHHPHHFQ
241	HHHSQHQQQRRSPASP PPPFTHRNAAFNQLPHLANNLNKPPSPWSSYQSPSPTPSSWS
301	PGGGGYGGWGGSGQRDHRRGLNGGITPLNSISPLKKNFASNHIQLQKYARPSSAFAPKSW
361	MEDSLNRADNIFPF

B

AA	#	%
S	50	13.3
P	41	10.9
G	35	9.3
A	32	8.5
Q	29	7.7
N	28	7.5
SUM	215	57.3

C

	This study	Hu et al. (2014)	Tsai et al. (2013)
Cpeb4 GT/GT	C57bl/6NTac X C57bl/6	C57bl/6NTac X C57bl/6	N/A
Cpeb4 Δ E2/ Δ E2	C57bl/6NTac X C57bl/6	N/A	C57bl/6
FlpE	C57bl/6	N/A	N/A
Protamine Cre	C57bl/6	N/A	C57bl/6

Figure S2, related to Figure 3

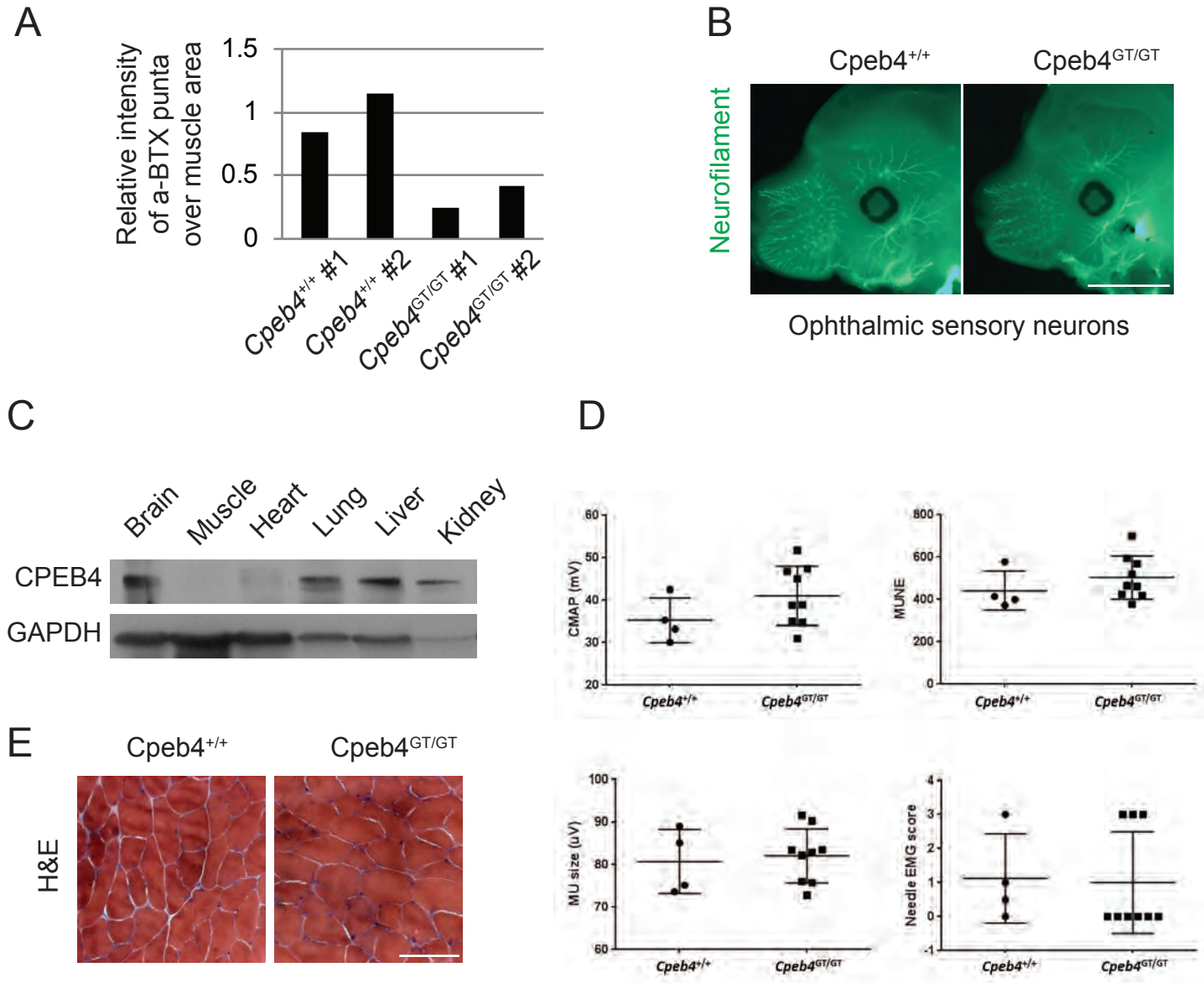


Figure S3, related to Figure 4

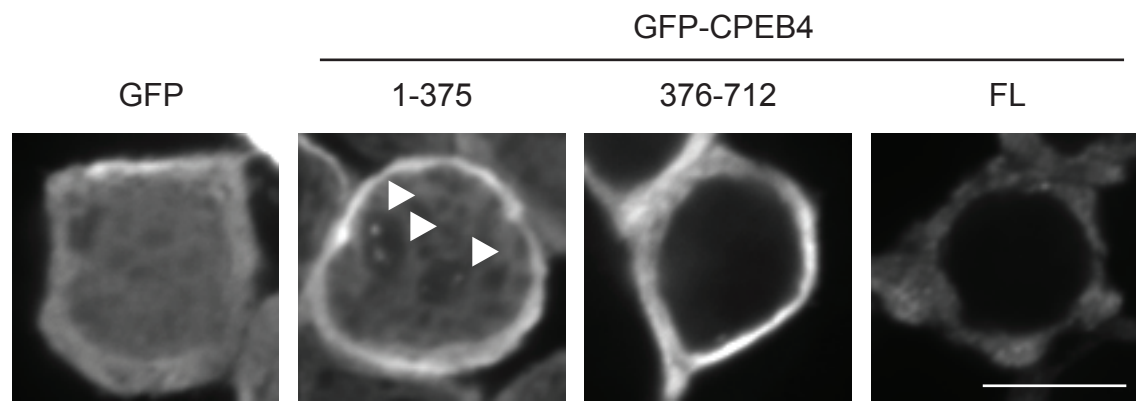


Figure S4, related to Figure 5

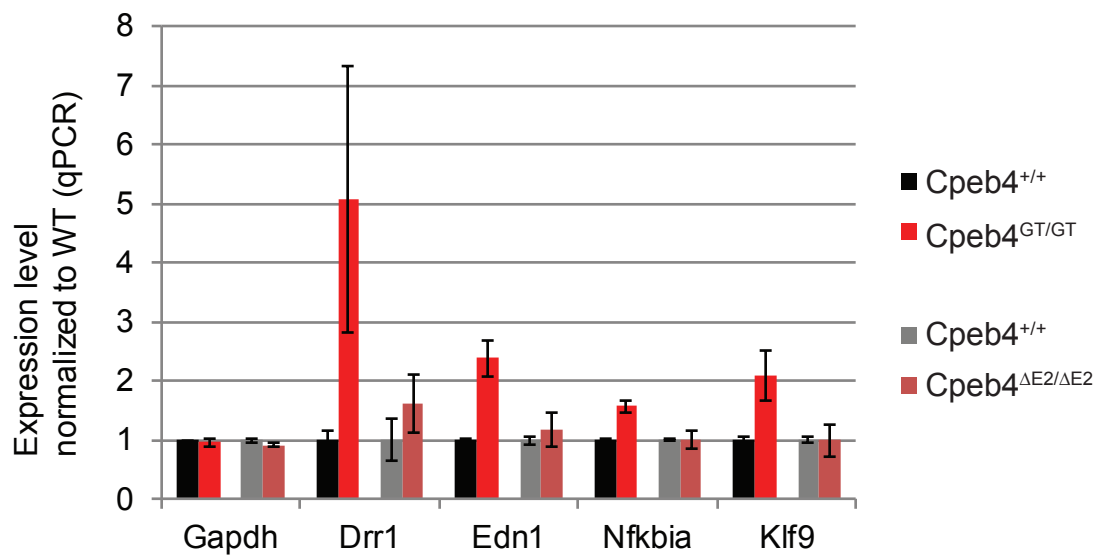
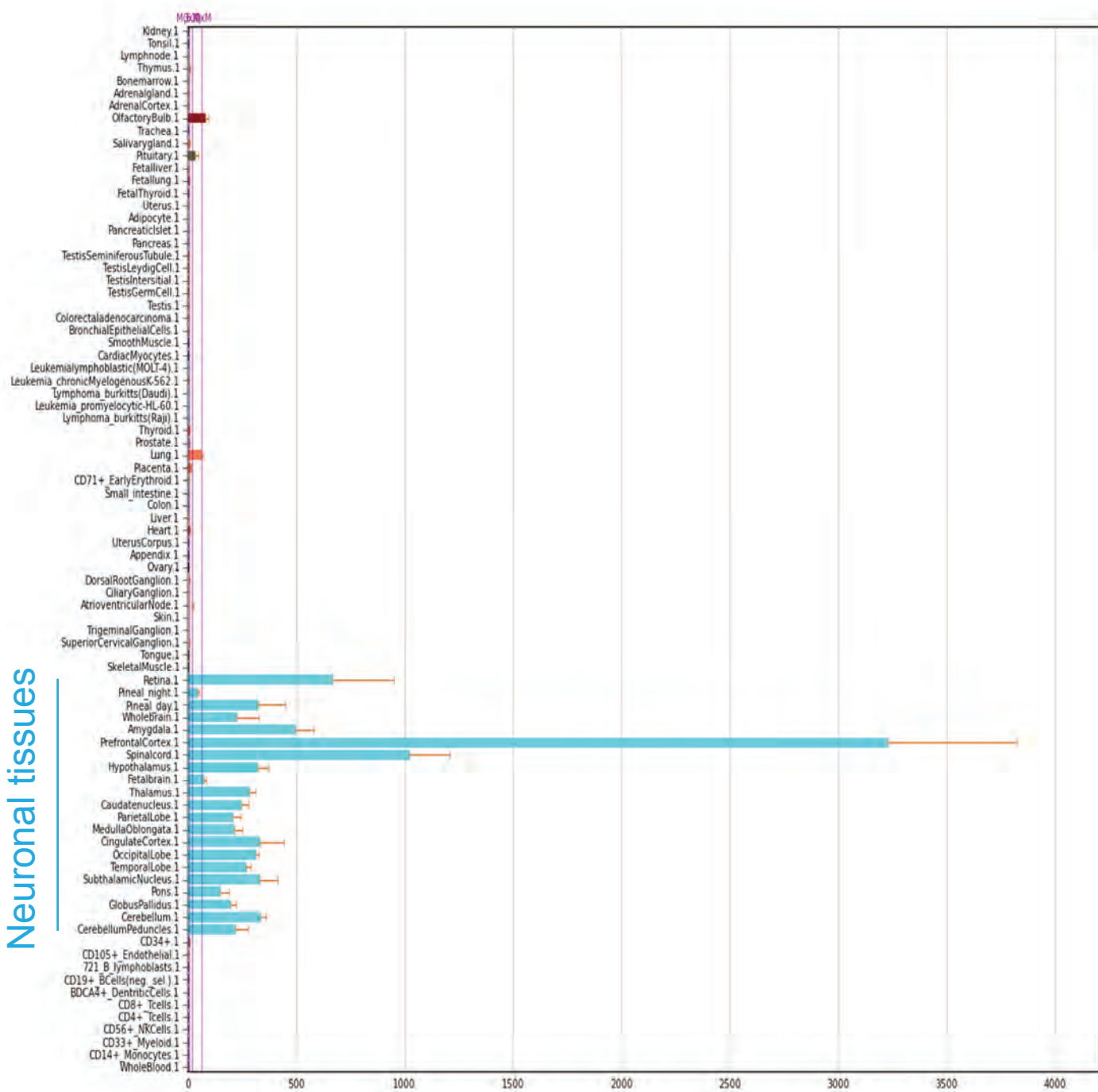


Figure S5, related to Figure 5

A



B

Reference	Disease	Accession #	Original study first author	Year	Species	Tissue Source
Li (2014)	ALS	GSE26927	Durrenberger	2012	Human	Cervical spinal cord
	ALS	GSE4595	Lederer	2007	Human	Motor cortex
	HD	GSE26927	Durrenberger	2012	Human	Ventral head of caudate nucleus
	PD	GSE26927	Durrenberger	2012	Human	Substantia nigra
	PD	GSE7621	Lesnick	2007	Human	Substantia nigra
	PD	GSE20333	Grunblatt	2004	Human	Substantia nigra
	PD	GSE20164	Hauser	2005	Human	Substantia nigra
Shao (2008)	SZ	N/A	Shao	2008	Human	Dorsolateral prefrontal cortex
	BPD	N/A	Shao	2008	Human	Dorsolateral prefrontal cortex
Murray (2010)	SMA	N/A	Murray	2010	Mouse	Spinal cord

Supplemental legends

Movie S1. Suckling behavior and mobility during nipple attachment test in *Cpeb4*^{+/+} and *Cpeb4*^{GT/GT} mouse pups at p0.

Movie S2. Gasping of *Cpeb4*^{GT/GT} pup at p0 (right).

Table S1. Differentially regulated genes in p0 *Cpeb4*^{GT/GT} mouse spinal cord.

Figure S1, related to figure 2. (A) Protein sequence of CPEB4 exon 1 and the amino acid composition. (B) The number and percentage of amino acid usage is summarized. (C) Genetic background of the mice used in this study, Hu et al. (2014) and Tsai et al. (2013).

Figure S2, related to figure 3. (A) Quantification of a-BTX puncta area over the muscle area of *Cpeb4*^{+/+} and *Cpeb4*^{GT/GT} diaphragms (scale relative to mean of WT). (B) Whole mount anti-neurofilament staining of e12.5 mouse face for ophthalmic sensory axon branching. (C) Western blot analysis of various mouse tissues probed with CPEB4 antibody. GAPDH is a loading control. (D) Electromyography (EMG) for sciatic nerve of 2 year old *Cpeb4*^{+/+} and *Cpeb4*^{GT/GT} mice to measure motor neuron degeneration. CMAP, measurement of compound muscle action potential. MUNE, motor unit number estimation. MU, motor unit. (E) H&E histology of tibialis anterior muscles in *Cpeb4*^{+/+} and *Cpeb4*^{GT/GT} mice.

Figure S3, related to figure 4. N2a cells transfected with GFP, GFP-CPEB4 residue 1-375, GFP-CPEB4 376-712, or GFP-CPEB4 full length (FL) were stained with GFP and FUS (nuclear protein) antibodies. These are magnified images of Fig. 4D.

Figure S4, related to figure 5. Quantitative RT-PCR of *Drrl*, *Edn1*, *Klf9*, and *Nfkbia* RNAs normalized to *Ppia* mRNA from p0 *Cpeb4*^{+/+} (gray) and *Cpeb4*^{ΔE2/ΔE2} (grayish red) spinal cord (mean ± SEM). Histograms for *Cpeb4*^{+/+} (black) and *Cpeb4*^{GT/GT} (red) were duplicated from Fig. 5B to show the relative expression levels.

Figure S5, related to figure 5. (A) Expression level of *Drrl* in various human tissues from BioGPS (<http://biogps.org>); GeneAtlas U133A, germa; probeset is 207547_s_at. (B) Summary of public gene expression data sets used in Fig. 5H.

Supplemental Experimental Procedures

Oligonucleotides sequences

Cpeb4 ^{GT/+}	fwd	5'-AGGACGTTGACATGCACTCACGGAGAGCTCACT-3'
Cpeb4 ^{GT/+}	rev	5'-CCTGCTTATATTCTGGCCTCAAGTTGTTAGTGACTATGTT-3'
Cpeb4 ^{ΔE2/ΔE2}	fwd	5'-CATAATTCATAGAGAGTGGAGGTCTATCAAATCAC-3'
Cpeb4 exon 1	rev	5'-CATGTCAGCCCTGGCTTGTT-3'
Cpeb4 exon 6	rev	5'-TGGTTTATCCTTGATGGTTGGACTTG-3'
Cpeb4 exon 10	rev	5'-CATTCTTCAGTCCAGCGGAATG-3'
Drr1	fwd	5'-TAGGACCACCCAAGGGACTTAGC-3'
Drr1	rev	5'-GGGACTAACAGAGTCACAGAGTATCAAGGT-3'
Gapdh	fwd	5'-AACGACCCCTTCATTGACCT-3'
Gapdh	rev	5'-TGGAAAGATGGTATGGGCTT-3'
FLAG tagged Drr1	fwd	5'- GCCTCCGGATCCAGCCTCCATGTACTCAGAGA-3' 5'-CGGTCCCGAATTCTCTGCTCACTTGTCTCGTCG
FLAG tagged Drr1	rev	TCCTTGTAGTCCAGTGCTCTTCCTCGCTGGT-3'
shRNA Drr1	fwd	5'-TGGCTGACATCGAGGGACTTCAAGAGA-3'
shRNA Drr1	rev	5'-TCGAGAAAAAAGGGCTGACATCGAGGG-3'
Ppia	fwd	5'-CTCCTCGAGCTGTTGCAGACAAAG-3'
Ppia	rev	5'-ACCCTGGCACATGAATCCTGGAA-3'
Edn1	fwd	5'-AGGCCATCAGCAATAGCATC-3'
Edn1	rev	5'-TTGTGCGTCAACTTCTGGTC-3'
Klf9	fwd	5'-CACATGAAATCTGCCACAG-3'
Klf9	rev	5'-CAAGGGGACCAAATGTTGAC-3'
Nfkbia	fwd	5'-ACCTGGTTTCGCTCTTGTG-3'
Nfkbia	rev	5'-TGGAGATTTCCAGGGTCAG-3'
45S	fwd	5'-GAGCTGGTGGTGGCGCTCC-3'
45S	rev	5'-CTGCCCTCCTCTCT-3'
18S 5junction	fwd	5'-GACGCTCCGCTCGCGCTCCTTACCT-3'
18S 5 junction	rev	5'-TAGACATGCATGGCTTAATCTTG-3'
18S 3 junction	fwd	5'-AGTCGTAACAAGGTTCCGTAGGT-3'
18S 3 junction	rev	5'-CCACAGTCTCCGTTAAT-3'
5.8S 5junction	fwd	5'-TACGACTCTTAGCGGTGGATCA-3'
5.8S 5junction	rev	5'-TCACATTAATTCTGCAGCTAGCT-3'
5.8S 3junction	fwd	5'-GAATTGCAGGACACATTGATCATC-3'
5.8S 3junction	rev	5'-GTCAACCGACGCTCAGA-3'
28S 5junction	fwd	5'-CTGACCGCGACCTCAGAT-3'
28S 5junction	rev	5'-TCCGCTGACTAATATGCTTAAATTCA-3'
Mature 18S	fwd	5'-GATGGTAGTCGCCGTGCC-3'
Mature 18S	rev	5'-GCCTGCTGCCTCCTTGG-3'
Mature 5.8	fwd	5'-ACTCGGCTCGTGCCTC-3'
Mature 5.8	rev	5'-CCGACGCTCAGACAGG-3'
Mature 28S	fwd	5'-GACGCGCATGAATGGA-3'
Mature 28S	rev	5'-TGTGGTTTCGCTGGATAGTAGGT-3'

Electrophysiological recordings

Electrophysiological recordings were done as previously described (Xia et al., 2010) on 2 year old mice. Mice were deeply anesthetized with isoflurane. Motor conduction studies and motor unit number estimate (MUNE) were performed using a portable electrodiagnostic system (Cardinal Synergy). For the MUNE recordings, the incremental technique was used (Shefner et al., 2006). After recording from each side, the animals were euthanized.

Quantification of a-BTX puncta

Images for whole mount diaphragm were stacked for maximum intensity and binary images of a-BTX positive area were analyzed for particle area (ImageJ).

Supplemental References

- Shefner, J.M., Cudkowicz, M., and Brown, R.H., Jr. (2006). Motor unit number estimation predicts disease onset and survival in a transgenic mouse model of amyotrophic lateral sclerosis. *Muscle & nerve* *34*, 603-607.
- Xia, R.H., Yosef, N., and Ubogu, E.E. (2010). Dorsal caudal tail and sciatic motor nerve conduction studies in adult mice: technical aspects and normative data. *Muscle & nerve* *41*, 850-856.